Fibonacci-like photonic structure for femtosecond pulse compression

L. N. Makarava,[1,2] M. M. Nazarov,[1] I. A. Ozheredov,[1] A. P. Shkurinov,[1]
A. G. Smirnov,[3] and S. V. Zhukovsky[4,2]
[1]*Department of Physics and International Laser Center, M. V. Lomonosov Moscow State University, Leninskie Gory, 119992, GSP-2, Moscow, Russia*
[2]*Institute of Molecular and Atomic Physics, National Academy of Sciences, Independence Avenue 70, 220072, Minsk, Belarus*
[3]*B. I. Stepanov Institute of Physics, National Academy of Sciences, Independence Avenue 68, 220072, Minsk, Belarus*
[4]*Physikalisches Institut, Universität Bonn, Nussallee 12, D-53115, Bonn, Germany*
(Received 25 October 2006; published 16 March 2007)

The compression of femtosecond laser pulses by linear quasiperiodic and periodic photonic multilayer structures is studied both experimentally and theoretically. We compare the compression performance of a Fibonacci and a periodic structure with similar total thickness and the same number of layers, and find the performance to be higher in the Fibonacci case, as predicted by numerical simulation. This compression enhancement takes place due to the larger group velocity dispersion at a defect resonance of the transmission spectrum of the Fibonacci structure. We demonstrate that the Fibonacci structure with the thickness of only 2.8 μm can compress a phase-modulated laser pulse by up to 30%. The possibility for compression of laser pulses with different characteristics in a single multilayer is explored. The operation of the compressor in the reflection regime has been modeled, and we show numerically that the reflected laser pulse is subjected to real compression: not only does its duration decrease but also its amplitude rises.

DOI: 10.1103/PhysRevE.75.036609 PACS number(s): 42.25.Bs, 42.25.Fx, 42.65.Ky, 73.20.Mf

I. INTRODUCTION

Nowadays most studied inhomogeneous physical systems are either periodic or random. However, there is also an intermediate class. As is known in mathematics, it is possible to establish a long-range order in space without the need of geometrical periodicity, and sometimes even without a short-range order. Several decades ago, such *deterministically aperiodic* systems got into the sphere of interest of physicists. In studying the phenomenon of Anderson localization of electrons in such systems, it was found that electrons in a one-dimensional (1D) quasiperiodic potential possess critical power-law-localized eigenstates, as opposed both to extended and to exponentially localized ones, as well as self-similar eigenvalue spectra (see [1,2] and references therein). Subsequent experimental results of Merlin and co-workers [3], where electron transport was studied in fabricated quasiperiodic Fibonacci heterostructures, encouraged further research in this intriguing area. The renormalization group method [1,2] was further developed [4] and used to study the 1D quasiperiodic problem in more detail, e.g., spectral clustering [4] and the diffusion properties [5]. Other studies, mainly numerical, include anomalous conductance [6] and resonance statistics [7], as well as correlation between the properties of eigenstates in a Fibonacci lattice and Fibonacci numbers [8]. The results for 1D problems turned out to be applicable to semiconductor superlattices [9]. Further experiments on Fibonacci structures followed, e.g., on synchrotron x-ray scattering and diffraction [10], photoexcited carrier transfer [11], and electron transport through narrow quasiperiodically modulated constriction [12].

Since the eigenvalue problem of a quantum mechanical system with a quasiperiodic 1D potential and the problem of classical wave propagation in a 1D multilayer structure are, to a certain extent, mathematically analogous, the above mentioned electronic properties are expected to be manifest for both acoustic and optical waves. The analysis of the energy spectrum of phonons in 1D quasicrystals revealed a Cantor-set-like structure of gaps in the short-wavelength regime [13,14]. Furthermore, many localized states corresponding to surface phonons have been found in the gaps [13], and self-similarity as well as nesting in the transmission spectra have been observed in the propagation of third sound through a superfluid Fibonacci structure [15,16].

The propagation of electromagnetic waves in quasiperiodic Fibonacci optical heterostructures (QFOHs) was studied as well. The renormalization-group-based theoretical investigations of a 1D quasiperiodic problem [17,18] confirmed the scaling and self-similar properties of the optical spectra, analogous to electronic ones. As regards to experimental studies of the quarter-wave dielectric multilayer thin-film QFOH, several groups [19,20] observed the scaling of the transmission coefficient with the increase of the stage of the Fibonacci sequence. Self-similarity was also noticed experimentally for the dispersion of SiO_2/TiO_2 QFOHs [21].

In some respects, QFOHs have proved to be advantageous over periodic optical heterostructures (POHs) and photonic random superlattices. For example, the authors [22] found that the enhancement of the second-harmonic (SH) generation in a QFOH is larger than that in a random structure, but smaller than in a POH. However, the efficiency of light conversion to the third harmonic (TH) in QFOHs is increased, compared with the two-step process in POHs [23]. This is due to two facts: first, the energy transfer from the fundamental to the SH and then TH fields are coupled with each other in the QFOH, this coupling leading to a one-step energy transfer. Second, the variation of a QFOH layer thickness allows one to adjust the nonlinear optical coefficients to obtain the most efficient TH generation.

The nonlinear properties of optical heterostructures can also be used to design a compact-sized compressor for laser

pulses. The periodic Bragg gratings with Kerr nonlinearity induced in optical fibers were first shown theoretically [24] and later experimentally [25] to have advantages over traditional methods of picosecond pulse compression. At wavelengths longer than 1.3 μm, such fibers can be used to compress laser pulses without an additional external grating or anomalous-dispersion delay line. A 1D POH of submillimeter size with relatively deep modulation of the refractive index facilitates compression in the visible spectrum. These structures were shown theoretically [26,27] to compress a picosecond pulse up to the duration of several optical cycles. The first experimental study in the femtosecond time range revealed a 15% decrease of chirped pulse duration in a POH of 4.8 μm thickness [28].

Since the effect of laser pulse compression in linear photonic structures is basically determined by the dispersion properties, namely, by group velocity dispersion (GVD), it can be expected that by adding more layers to the POH, the compression effect can be increased. However, this is inevitably accompanied by an increase of the total thickness of the structure, which is undesirable.

Another possibility would be to try changing the multilayer geometry from periodic to nonperiodic. In some cases such as the chirped quasi-phase-matched (QPM) gratings this is known to improve the compressor performance. If the aperiodicity of such a grating exactly matches the chirp of the incoming optical pulse, then the generated transform-limited SH pulse can be effectively compressed [29]. However, the efficiency of SH generation (and, consequently, the amplitude of the compressed pulse) is relatively low, although still higher than in periodic QPM gratings. Orienting a chirped linear POH at Brewster's angle allows compression of incident picosecond pulses up to a single optical cycle [30], albeit at considerably larger structure thickness of about 100 μm.

Structures with a higher degree of aperiodicity are known to possess even stronger GVD. A very recent work [31] reports good results on pulse chirp compensation in a POH where nonperiodicity is manifest in the form of incorporated coupled defects, which can be used to design an ultracompact delay line for femtosecond pulses [32].

As we had shown earlier [33], the QFOHs are also known to have a higher GVD, which makes them advantageous as a pulse compressor compared to a POH with a similar total thickness. In this paper we focus on analyzing the influence of topology-related effects on femtosecond chirped pulse compression in thin-film photonic structures. In particular, we compare the performance of QFOHs and POHs with similar thickness and report the former to be better. We thus confirm our earlier estimations experimentally and report double-pass compression efficiency of up to 30% for a structure as thin as 2.8 μm, which exceeds what has been reported in [31]. We also analyze the effects related to the pulse chirp sign, as well as double-pass vs single-pass compression regime.

The plan of this paper is as follows. First, we describe the design and fabrication of multilayer photonic structures. Then we show the theoretical background and numerically simulate the shape of the femtosecond laser pulse after its transmittance through the photonic structures. After that we describe the experimental setup and the measurement techniques, followed by the experimental results on chirped femtosecond laser pulse compression by binary QFOHs and POHs. These results are discussed in the final sections of the paper.

II. FIBONACCI AND PERIODIC STRUCTURE DESIGN AND FABRICATION

We study and compare two multilayer structures, which are similar in parameters but different in the geometrical organization of the constituent layers. Both samples are made from high-index ZnS (n_H=2.3) and low-index Na_3AlF_6 (n_L =1.25) layers (labeled further as H and L layers, respectively). The thickness of each layer is chosen to satisfy the condition $d_i=3\lambda/4n_i$ ($i=H,L$) for the reference wavelength λ=815 nm. From the point of view of optical spectra, this is equivalent to the usual quarter-wave condition ($d_i=\lambda/4n_i$) for the reference wavelength $\lambda \rightarrow 3\lambda$, and it was so chosen to make the van Hove fixed points occur more frequently in the spectra. This leads to "compression" of the spectrum on the frequency scale, which in turn increases the GVD without increasing the number of layers in the structure. The whole stack is deposited on a glass substrate (S) with a thickness of 2 mm.

The POH is a four-period, eight-layer stack, which can be coded as $\{HLHLHLHLS\}$ and will be further referred to as a P_4 structure. Its total thickness is 3.0 μm.

The Fibonacci quasiperiodic sequence is typically formed by recurrently stacking two adjacent sequence members to create the next one. This can be expressed as $F_{j+1}=\{F_{j-1}F_j\}$ for $j \geqslant 1$, with $F_0=\{L\}$ and $F_1=\{H\}$. The same can be achieved by recurrently acting on the initiator $F_0=\{L\}$ with a simple set of substitution rules: $L \rightarrow H$, $H \rightarrow LH$. The sequence then takes the form $F_2=\{LHS\}$, $F_3=\{HLHS\}$, $F_4=\{LHHLHS\}$, $F_5=\{HLHL\mathbf{HH}LHS\}$, and so on. The latter consists of eight layers, just like P_4, and is also close in total thickness (2.8 μm). So the structure F_5 is used as the QFOH to be compared in its compression properties with the POH P_4. Both structures were fabricated by using cathode-anode method of vacuum evaporation.

The measured normal-incidence optical density of the samples under study is shown in Fig. 1. The spectra were obtained using a Hitachi 356 spectrophotometer. The maxima of optical density in Fig. 1 correspond to relatively wide low-transmission regions called photonic band gaps (PBGs), which are an optical analogy to an electronic band gap in a semiconductor, as put forth in [34]. The transmission spectrum of the QFOH also contains forbidden frequency regions (*pseudo band gaps*), similar in properties to the band gaps of POHs [19,20,35,36]. (For brevity we will refer to the band gaps in both QFOHs and POHs as PBGs.) In contrast to a POH, a QFOH can have more than one PBG in one spectral period $[4m\pi c/3\lambda;4(m+1)\pi c/3\lambda]$, the number of the gaps increasing with the growth of QFOH generation [20]. (As the light waves are critically localized at the resonances of a QFOH, in contrast to the band edge resonances of a POH, which usually support delocalized modes, those Fi-

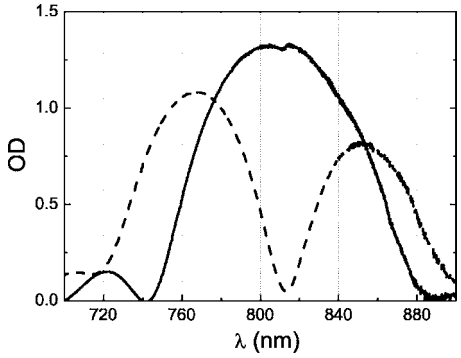

FIG. 1. Measured spectra of optical density (OD) ($\log_{10} 1/T$, where T is transmission) for experimental samples: dashed line for QFOH F_5 and solid line for POH P_4.

bonacci resonances can exhibit mode beating [37].)

In particular, the QFOH F_5 has two PBGs in the wavelength range of interest (see Fig. 1). We will call them the short-wave and the long-wave PBG, respectively. The dip of optical density between these two PBGs—a *defect resonance* associated with disorder of geometrical periodicity—is the main spectral peculiarity of the QFOH F_5.

III. THEORETICAL BACKGROUND AND NUMERICAL SIMULATION

We examine a POH and a QFOH, in which the materials of the constituent layers do not possess the Kerr effect. Earlier [38] it was speculated that a linear dispersive medium could compress an optical pulse provided that the pulse phase is modulated. We shall deal with a phase-modulated laser pulse of Gaussian type:

$$E(t)|_{x=0} = A \exp\left(-\frac{1}{2}(\tau_0^{-2} + i\alpha_0)t^2\right)\exp(i\omega_0 t), \qquad (1)$$

where τ_0 is the characteristic duration of the pulse (note that we consider a pulse that is not a transform limited pulse and can be compressed), α_0 is the rate of frequency modulation, which is commonly referred to as *chirp*, and ω_0 is the central frequency. In the framework of the slowly varying envelope approximation, taking into account the second-order dispersion, the spatial evolution of pulse duration is described in the following manner [38]:

$$\tau(x) = \tau_0 \sqrt{(1 - \alpha_0\kappa_2 x)^2 + \left(\frac{\kappa_2 x}{\tau_0^2}\right)^2}. \qquad (2)$$

Here $\kappa_2 = \partial^2\kappa/\partial\omega^2$ is the dispersion of the group velocity, $v_{gr} = \partial\omega/\partial\kappa$. As seen from Eq. (2), in the case of $\alpha_0\kappa_2 < 0$, the chirped laser pulse is stretched while propagating through a structure. If, however, $\alpha_0\kappa_2 > 0$, the duration of the initially chirped pulse decreases, achieves its minimum, and then increases again. The minimum duration of such a phase-modulated Gaussian light pulse is thus defined as [38]

$$\tau_{min} = \frac{\tau_0}{\sqrt{1 + (\alpha_0\tau_0^2)^2}}. \qquad (3)$$

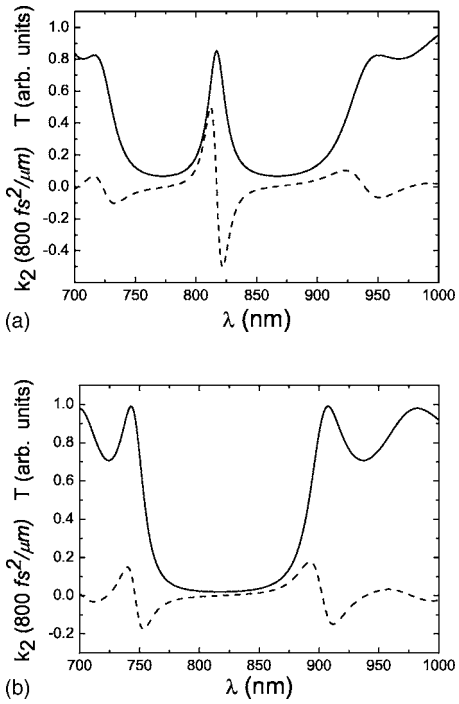

FIG. 2. Calculated transmission T (solid lines) and GVD κ_2 (dashed lines) spectra of fifth-generation QFOH F_5 (a) and eight-layer POH P_4 (b).

For this case of maximum compression, the pulse becomes transform limited and its duration τ_{min} is related to the spectral width $\Delta\omega$ as $\tau_{min}\Delta\omega = 0.44$ (for a Gaussian shape pulse). The duration τ_{min} is achieved at a distance [38]

$$L_{compr} = \frac{(\alpha_0\tau_0^2)^2}{\alpha_0\kappa_2[1 + (\alpha_0\tau_0^2)^2]}. \qquad (4)$$

As can be seen from Eq. (3), the chirped pulse duration is decreased significantly provided that $|\alpha_0\tau_0^2| > 1$, which means physically that phase modulation has to be faster than amplitude decay. The chirped-pulse compression efficiency attainable at the distance L_{compr} is proportional to the parameter $|\alpha_0\tau_0^2|$, whose physical meaning is the spectral width ratio between the pulse in question and the transform-limited pulse of the same duration.

Let us point out that the condition necessary for pulse compression, namely, $\alpha_0\kappa_2 > 0$, is achieved when the GVD of the structure is matched in sign with the pulse chirp α_0. So, e.g., an initially negatively chirped ($\alpha_0 < 0$) laser pulse can be compressed if its spectrum corresponds to a frequency range where the GVD is negative. As can be seen from transfer-matrix numerical calculations (see Fig. 2), such a negative GVD is present at the high-frequency (or short-wave) edge of the PBG for both F_5 and P_4.

To study the propagation of chirped optical pulses in PBG structures numerically, we have used the finite-difference Lax-Wendroff scheme with the initialization proposed in [39]. Both pulse duration and pulse profile distortion can be analyzed in this way.

First we compare the duration of the chirped laser pulses passed through the QFOH F_5 and POH P_4, as described

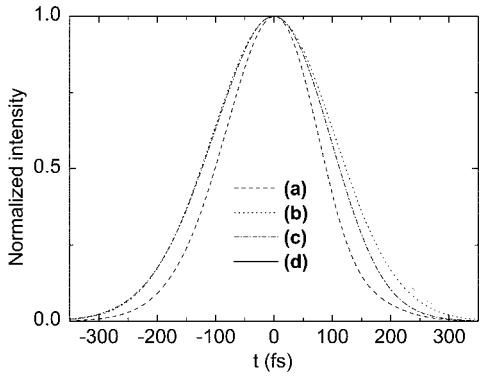

FIG. 3. Calculated profiles of negatively chirped laser pulses transmitted through QFOH and POH: (a) QFOH, λ_0=856 nm (short-wave edge of long-wave gap); (b) QFOH, λ_0=754 nm (short-wave edge of short-wave gap); (c) POH, λ_0=785 nm (short-wave edge); (d) profile of incoming pulse.

above, at the short-wave edges of the photonic band gaps of the transmission spectrum. The simulation predicts that the negatively chirped laser pulse with $|\alpha_0\tau_0^2|$=4.6 and central wavelength λ_0=856 nm corresponding to the short-wave edge of the long-wave PBG of the F_5 transmission spectrum [see Fig. 2(a)] is compressed more strongly than the pulse with λ_0=754 nm corresponding to the short-wave edge of the short-wave PBG [Figs. 3(a) and 3(b)]. In addition, the compression of the laser pulse with λ_0=856 nm by the QFOH F_5 exceeds the compression of the pulse with the same spectral width in the P_4 for λ_0=785 nm corresponding to the short-wave gap edge [Figs. 3(a) and 3(c)]. This enhancement of compression occurs because the QFOH has a greater value of GVD at this wavelength compared both with other band edges of F_5 and with P_4 (Fig. 2). Such a tendency is also observed for the positively chirped laser pulse whose central wavelength corresponds to the PBG long-wave edges of the QFOH and the POH.

Besides compression of a transmitted pulse, photonic multilayers can also compress pulses in the reflection regime, which is advantageous because smaller attenuation in the pulse amplitude is expected. In Fig. 4 we compare the compression of chirped laser pulses reflected from the QFOH F_5 and the POH P_4. The reflected pulse has a much greater amplitude than the transmitted one [Figs. 4(1a) and 4(1c)]. As with the transmitted pulse, it can be seen that the positively chirped incoming laser pulse with $|\alpha_0\tau_0^2|$=4.74 is compressed better when reflected from the QFOH than from the POH, which can be seen clearly if the profiles are normalized and their maxima are superimposed [Figs. 4(2a) and 4(2b)]. The central wavelength of the incoming pulse is taken at the long-wave edge of the PBG: λ_0=810 nm corresponding to the long-wave edge of the short-wave gap of the F_5 transmission spectrum and λ_0=856 nm for P_4 (see Fig. 2).

In addition, the amplitude of the pulse reflected from F_5 is greater than that reflected from P_4, as well as greater than that of the incident pulse [Figs. 4(1a), 4(1b), and 4(1d)].

IV. EXPERIMENTAL SETUP

Our experimental system (Fig. 5) is based on a commercial mode-locked Ti:sapphire laser (Tsunami, Spectra Physics) which typically gives 100 fs duration pulses with 1.4 W average power and 80 MHz repetition rate. The laser wavelength can be tuned in the range from 710 to 990 nm and the pulse spectrum bandwidth in the range from 5 to 30 nm full width at half maximum.

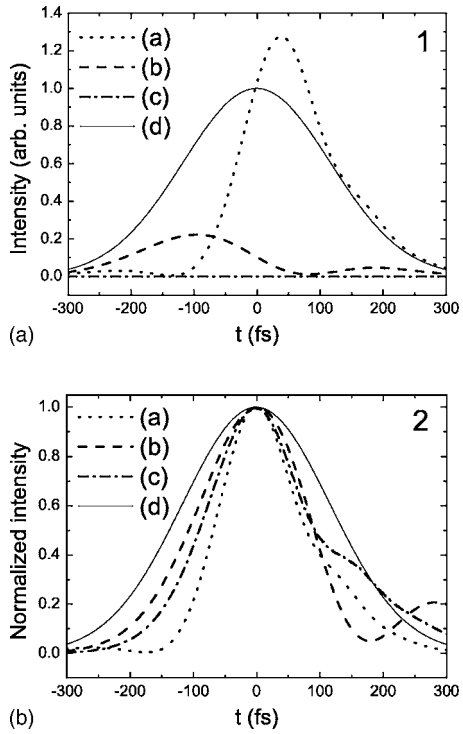

FIG. 4. (1) Profile of an incident positively chirped laser pulse (d) along with the calculated profiles of such a pulse reflected from QFOH F_5 (a) and from POH P_4 (b) and transmitted through QFOH F_5 (c). (2) Same profiles as in (1) normalized and shifted so that all maxima become superimposed in order to facilitate the pulse width comparison.

To change the sign and the value of a chirp and, consequently, the parameter $|\alpha_0\tau_0^2|$ in the range from 2.7 to 5, as

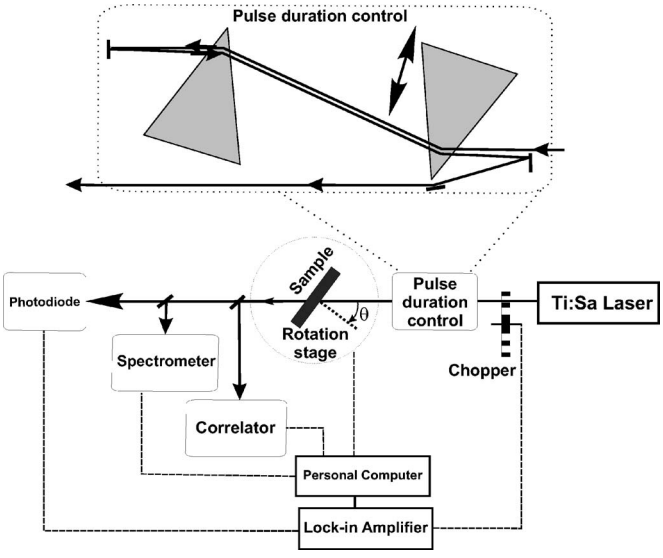

FIG. 5. Experimental setup scheme.

well as the pulse duration τ_0 from 70 to 300 fs, we used a system of pulse duration control (external compressor), which consists of a pair of SF-10 prisms and three dielectric mirrors (see Fig. 5). By moving the prism across the beam and correspondingly increasing (decreasing) the amount of glass inside the optical path of the pulse we introduce a positive (negative) chirp of the pulse. This method of changing the pulse duration does not alter its spectrum. The pulse spectral bandwidth determines the minimal pulse duration (for zero GVD and chirp value).

The pulse duration was measured by a second-order interferometric autocorrelator (AA 10DM, Avesta), and the spectrum was measured by a spectrometer (SP-500i, ARC) and a cooled charge-coupled device camera system (SPEC 10, PI-Acton). The average power of the pulse was measured by a calibrated photodiode, using lock-in amplifier techniques (SR-810 SRS). To modulate the incident beam, we used an optical chopper (SR-540, SRS). The polarization of laser radiation was set to p (the electric field is in the plane of incidence). To control the polarization state, we used a $\lambda/2$ plate and a Glan-Taylor polarizer.

The samples were mounted on the rotary part of a goniometer. The goniometer rotation axis was controlled to be in the plane of the sample. The sample could be moved out of the beam path and placed back with a translation stage [28].

In experiments, we need to tune the laser wavelength relative to the PBG position. By changing the incident angle of laser radiation θ, we change the projection of the light wave vector on the reciprocal lattice vector of the structure. This moves the PBG location relative to the laser wavelength, allowing us to scan the slopes of the PBG while making sure that the pulse duration and its spectral bandwidth remain constant.

The setup has allowed us to study both temporal and spectral properties of the incident and transmitted radiation for the QFOH and POH vs the angle θ. We measured both the duration and the spectral profile of the pulses. The measurements of pulse parameters were made just outside the sample. In the experiments, the incidence angle was changed in the range from 0 to 70°, with the accuracy of two angular minutes.

V. EXPERIMENTAL STUDIES OF PULSE COMPRESSION

In this section we analyze our experimental results. We carried out several sets of experiments. In each experimental set, we analyze the temporal and spectral properties of the radiation incoming on the QFOH and POH and transmitted through them vs the incidence angle θ. The laser pulse wavelength was fixed at $\lambda_0=787$ nm.

In the first experimental set, we measured the transmitted pulse compression ratio ($\eta=\tau/\tau_0$ where τ is the duration of the transmitted pulse and τ_0 is the duration of the incoming one, so $\eta>1$ and $\eta<1$ correspond to pulse stretching and compression, respectively) vs the incidence angle θ for the QFOH F_5. The spectral width and duration of the incident pulse were $\Delta\lambda_0=18$ nm and $\tau_0=160$ fs. The experimental conditions were chosen to ensure the positive chirp sign of the femtosecond pulse incoming on the sample. The chirp parameter calculated from Eq. (3) was equal to $|\alpha_0\tau_0^2|=4.4$.

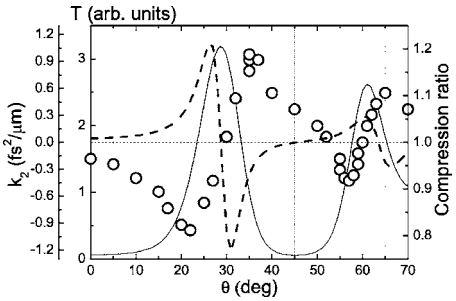

FIG. 6. Measured compression ratio $\eta=\tau/\tau_0$ (circles) and relative intensity T of transmitted positively chirped pulses (solid line) for the QFOH F_5 vs the incident angle θ, along with calculated value κ_2 (GVD) (dashed line). Compression is achieved where $\eta<1$.

The results of the measurements are shown in Fig. 6 along with the calculated value of κ_2 (GVD).

The second set of experiments was conducted to compare the compression efficiency of positively and negatively chirped incoming pulses. The wavelength of the laser pulses was $\lambda_0=787$ nm and the incident pulse duration was $\tau_0=140$ fs. The spectral width and the characteristic parameter were $\Delta\lambda_0=14$ nm and $|\alpha_0\tau_0^2|=3.7$, respectively. The results of this experimental set are shown in Fig. 7.

In the third experimental set we compared the compression ratio of positively chirped femtosecond pulses by the QFOH F_5 and POH P_4. The results are shown in Fig. 8. The incoming laser pulse has the same parameters as in the first experimental set.

The fourth experimental set is devoted to the measurements of the efficiency of positively chirped pulse compression after its double pass through the QFOH. In this regime we installed an aluminum mirror behind the QFOH. We measured the pulse duration both in single-pass and in double-pass transmission mode, the latter achieved due to reflection from the mirror and subsequent second transmission through the QFOH. The double-pass beam was filtered out from the reflected beam by spatial separation. The incident pulse was taken with the following parameters: $\lambda_0=787$ nm, $\tau_0=165$ fs, $\Delta\lambda_0=19$ nm, and $|\alpha_0\tau_0^2|=4.7$. The experimental results are shown in Fig. 9.

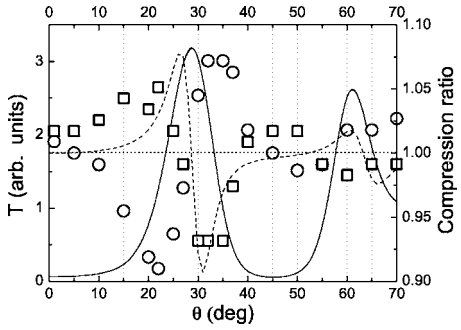

FIG. 7. Measured compression ratio for opposite-sign chirped pulses transmitted through the QFOH F_5 vs the incident angle θ. Circles and squares denote results for positive and negative sign of optical pulse chirp, respectively. As in Fig. 6, the solid line stands for the measured relative intensity T of the transmitted beam, and the dashed line represents calculated GVD κ_2.

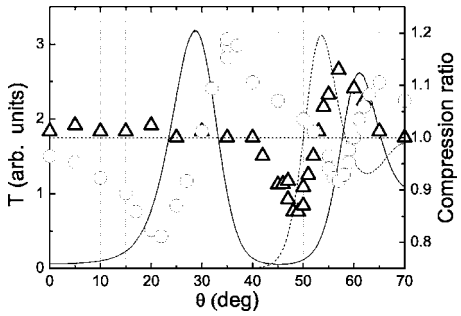

FIG. 8. For POH P_4, measured efficiency of positively chirped pulse compression (triangles) and transmitted relative intensity (dashed line) vs the incident angle. As in Fig. 6, the circles and the solid line denote results for compression ratio and transmitted relative intensity T for QFOH F_5, respectively.

VI. DISCUSSION

Our simulations as well as experimental results show that the QFOH can function as an efficient, compact-sized compressor of chirped femtosecond laser pulses. The efficient compression is found to occur at the corresponding edges of the PBG of the QFOH F_5, as predicted in the GVD simulations [33]. In the case of a positively chirped pulse, the most efficient compression is revealed in the experiment to be achieved near incidence angles $\theta=22°$ and 57° (Fig. 6), i.e., when the pulse central wavelength corresponds to long-wave edges of both PBGs of the QFOH. The negatively chirped femtosecond pulses are compressed at the opposite edges of the gaps at $\theta=34°$ and 60° (Fig. 7), where κ_2 has the opposite sign.

For the fifth-generation QFOH, there are two angular ranges in which the maximum level of the compression efficiency differs by two times (Fig. 7). The number of such angular ranges for any QFOH corresponds to the number of PBGs in the transmission spectra. The presence of several compression ranges in QFOH allows one to control the duration of different laser pulses by using a single compressor. The same QFOH could also be used as a compressor for both positively and negatively chirped pulses.

The experiments confirmed our expectations that, due to the higher GVD at the defect resonance in the transmission spectrum (Fig. 2), the QFOH is more effective for pulse compression compared to the POH with the same number of layers (Fig. 8). Note that the shape of the angular dependence of the compression qualitatively agrees very well with what has recently been reported for a single edge of the defect state of a POH with embedded coupled defects [31].

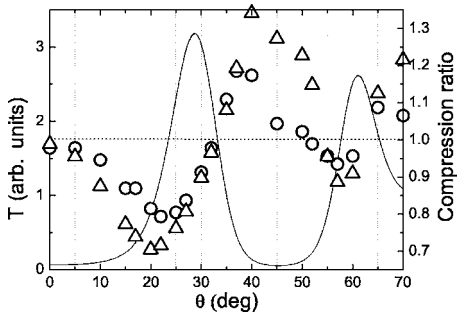

FIG. 9. Compression ratio for single-pass (circles) and double-pass (triangles) transmission through the QFOH F_5 vs the incident angle. The solid line, as in Fig. 6, indicates the transmittance T for the pulses through the QFOH F_5 in the single-pass regime.

In double-pass transmission mode, the pulse is compressed by about 30% by the QFOH (see Fig. 9). As a drawback, the amplitude of the transmitted pulse decreases drastically with each additional pass. Our simulations demonstrate that an efficient compression of the femtosecond pulses with decreased attenuation is possible if the pulse is reflected from (rather than transmitted through) the QFOH (Fig. 4), to be verified in a forthcoming study.

It should be noted that the optimal compression is achieved when the spectral width of the pulse matches that of the PBG edge [33], which is about 40 nm for the QFOH F_5 (see Fig. 1). The laser pulses used in our experiment only amount to half as much (about 20 nm). Nevertheless, even under such nonoptimal physical conditions, the QFOH compresses the chirped laser pulses by 20–30 % and better than the POH. Under optimal conditions, the QFOH could compress the chirped laser pulses even more strongly [33].

VII. CONCLUSIONS

In conclusion we have shown both numerically and experimentally the possibility of chirped femtosecond pulse compression by an ultrathin (2.8 μm) quasiperiodic Fibonacci optical heterostructure. The fifth-generation QFOH is seen to compress chirped pulses better than a periodic optical heterostructure equivalent both in the number of layers and in total thickness. This stronger compression occurs near the defect resonance of the transmission spectrum of the QFOH due to stronger dispersion. Compression of a chirped femtosecond pulse by as much as 30% has been demonstrated experimentally in the double-pass transmission mode. The presence of several band gaps in the transmission spectrum of the QFOH makes it possible to design a device for pulse duration control for both negatively and positively chirped laser pulses in a wide temporal range, based on only one photonic quasicrystal. Further regimes of QFOH compressor operation, such as using the reflected pulse, have been numerically considered. As the simulations have illustrated, the reflected laser pulse is subjected to real compression: not only does its duration decrease but its amplitude also rises.

ACKNOWLEDGMENTS

The authors acknowledge Professor A. V. Lavrinenko for his contribution to the numerical modeling of complex multilayer media, as well as for fruitful and stimulating discussions. Th authors are also grateful to the Belarusian Company "Optoelectronic systems" in Minsk for the sample preparation. The work was supported in part by RFBR (Grant Nos. 05-02-17298 and 05-03-32877). One of us the authors (S.V.Z.) wishes to acknowledge partial support of the Deutsche Forschungsgemeinschaft (DFG SPP 1113).

[1] M. Kohmoto, L. Kadanoff, and C. Tang, Phys. Rev. Lett. **50**, 1870 (1983).
[2] S. Ostlund and R. Pandit, Phys. Rev. B **29**, 1394 (1984).
[3] R. Merlin, K. Bajema, R. Clarke, F.-Y. Juang, and P. K. Bhattacharya, Phys. Rev. Lett. **55**, 1768 (1985).
[4] Q. Niu and F. Nori, Phys. Rev. Lett. **57**, 2057 (1986).
[5] M. Kohmoto and J. R. Banavar, Phys. Rev. B **34**, 563 (1986).
[6] J. B. Sokoloff, Phys. Rev. Lett. **58**, 2267 (1987).
[7] F. Steinbach, A. Ossipov, T. Kottos, and T. Geisel, Phys. Rev. Lett. **85**, 4426 (2000).
[8] X. Huang and Ch. Gong, Phys. Rev. B **58**, 739 (1998).
[9] E. Diez, F. Dominguez-Adame, E. Macia, and A. Sanchez, Phys. Rev. B **54**, 16792 (1996).
[10] J. Todd, R. Merlin, R. Clarke, K. M. Mohanty, and J. D. Axe, Phys. Rev. Lett. **57**, 1157 (1986).
[11] A. A. Yamaguchi, T. Saiki, T. Tada, T. Ninomiya, K. Misawa, and T. Kobayashi, Solid State Commun. **75**, 955 (1990).
[12] S. Katsumoto, N. Sano, and S. Kobayashi, Solid State Commun. **85**, 223 (1993).
[13] F. Nori and J. P. Rodriguez, Phys. Rev. B **34**, 2207 (1986).
[14] D. C. Hurley, S. Tamura, J. P. Wolfe, K. Ploog, and J. Nagle, Phys. Rev. B **37**, 8829 (1988).
[15] K. Kono, S. Nakada, Y. Narahada, and Y. Ootuka, J. Phys. Soc. Jpn. **60**, 368 (1991).
[16] K. R. Atkins and I. Rudnick, in *Progress in Low Temperature Physics*, edited by C. J. Gorter (North-Holland, Amsterdam, 1970), p. 37.
[17] M. Kohmoto, B. Sutherland, and K. Iguchi, Phys. Rev. Lett. **58**, 2436 (1987).
[18] K. Iguchi, Mater. Sci. Eng., B **15**, L13 (1992).
[19] L. Chow and K. H. Guenther, J. Opt. Soc. Am. A **10**, 2231 (1993).
[20] W. Gellermann, M. Kohmoto, B. Sutherland, and P. C. Taylor, Phys. Rev. Lett. **72**, 633 (1994).
[21] T. Hattori, N. Tsurumachi, S. Kawato, and H. Nakatsuka, Phys. Rev. B **50**, 4220 (1994).
[22] J. Feng, Y. Y. Zhu, and N. B. Ming, Phys. Rev. B **41**, 5578 (1990).
[23] S. N. Zhu, Y. Y. Zhu, and N. B. Ming, Science **278**, 843 (1997).
[24] H. G. Winful, Appl. Phys. Lett. **46**, 527 (1985).
[25] B. J. Eggleton, R. E. Slusher, C. M. de Sterke, P. A. Krug, and J. E. Sipe, Phys. Rev. Lett. **76**, 1627 (1996).
[26] N. I. Koroteev, S. A. Magnitskii, A. V. Tarasishin, and A. M. Zheltikov, Opt. Commun. **159**, 191 (1999).
[27] R. A. Vlasov and A. G. Smirnov, Phys. Rev. E **61**, 5808 (2000).
[28] A. V. Andreev, A. V. Balakin, I. A. Ozheredov, A. P. Shkurinov, P. Masselin, G. Mouret, and D. Boucher, Phys. Rev. E **63**, 016602 (2000).
[29] M. A. Arbore, O. Macro, and M. M. Fejer, Opt. Lett. **22**, 865 (1997).
[30] G. Steinmeyer, Opt. Express **11**, 2385 (2003).
[31] A. Belardini, A. Bosco, G. Leahu, M. Centini, E. Fazio, C. Sibilia, M. Bertolotti, S. Zhukovsky, and S. V. Gaponenko, Appl. Phys. Lett. **89**, 031111 (2006a).
[32] A. Belardini, O. Buganov, G. Leahu, A. Bosco, M. Centini, E. Fazio, C. Sibilia, M. Bertolotti, S. Zhukovsky, and S. V. Gaponenko, J. Optoelectron. Adv. Mater. **8**, 2015 (2006b).
[33] L. N. Makarava, A. V. Lavrinenko, and S. V. Zhukovsky, in *Proceedings of the Fourth ICTON and ESPC, Warsaw, 2002* (IEEE, Warsaw, 2002), Vol. 2, p. 140.
[34] J. D. Joannopoulos, P. R. Villeneuve, and S. Fan, Nature (London) **386**, 143 (1997).
[35] E. Macia, Appl. Phys. Lett. **73**, 3330 (1998).
[36] C. Sibilia, P. Masciulli, and M. Bertolotti, Pure Appl. Opt. **7**, 383 (1998).
[37] L. Dal Negro, C. J. Oton, Z. Gaburro, L. Pavesi, P. Johnson, A. Lagendijk, R. Righini, M. Colocci, and D. Wiersma, Phys. Rev. Lett. **90**, 055501 (2003).
[38] S. A. Akhmanov, V. A. Vyslouch, and A. S. Chirkin, *Optics of Femtosecond Laser Pulses* (AIP, New York, 1992).
[39] A. G. Smirnov, Opt. Commun. **158**, 343 (1998).